





# The effect of intrathecal recombinant arylsulfatase A therapy on structural brain magnetic resonance imaging in children with metachromatic leukodystrophy

Samuel Groeschel<sup>1</sup>  | Shanice Beerepoot<sup>2,3,4</sup>  | Lucas Bastian Amedick<sup>1</sup> | Ingeborg Krägeloh-Mann<sup>1</sup> | Jing Li<sup>5</sup> | David A. H. Whiteman<sup>5</sup>  | Nicole I. Wolf<sup>2</sup> | John D. Port<sup>6</sup> 

<sup>1</sup>Department of Pediatric Neurology, University Children's Hospital Tübingen, Tübingen, Germany

<sup>2</sup>Amsterdam Leukodystrophy Center, Department of Child Neurology, Emma Children's Hospital, Amsterdam University Medical Centers, Vrije Universiteit and Amsterdam Neuroscience—Cellular and Molecular Mechanisms, Vrije Universiteit, Amsterdam, Netherlands

<sup>3</sup>Center for Translational Immunology, University Medical Center Utrecht, Utrecht, Netherlands

<sup>4</sup>Princess Máxima Center for Pediatric Oncology, Utrecht, Netherlands

<sup>5</sup>Takeda Development Center Americas, Inc., Lexington, Massachusetts, USA

<sup>6</sup>Department of Radiology, Mayo Clinic, Rochester, Minnesota, USA

## Correspondence

Samuel Groeschel, Department of Neuropediatrics, University Children's Hospital Tübingen, 1 Hoppe-Seyler-Straße, 72076 Tübingen, Germany. Email: [samuel.groeschel@med.uni-tuebingen.de](mailto:samuel.groeschel@med.uni-tuebingen.de)

## Funding information

Shire, Grant/Award Numbers: NCT00681811, NCT00633139, NCT01887938, NCT00418561, NCT01510028; Takeda Development Center Americas, Inc

## Abstract

This study aimed to evaluate the effect of intrathecal (IT) recombinant human arylsulfatase A (rhASA) on magnetic resonance imaging (MRI)-assessed brain tissue changes in children with metachromatic leukodystrophy (MLD). In total, 510 MRI scans were collected from 12 intravenous (IV) rhASA-treated children with MLD, 24 IT rhASA-treated children with MLD, 32 children with untreated MLD, and 156 normally developing children. Linear mixed models were fitted to analyze the time courses of gray matter (GM) volume and fractional anisotropy (FA) in the posterior limb of the internal capsule. Time courses for demyelination load and FA in the centrum semiovale were visualized using locally estimated scatterplot smoothing regression curves. All assessed imaging parameters demonstrated structural evidence of neurological deterioration in children with MLD. GM volume was significantly lower at follow-up (median duration, 104 weeks) in IV rhASA-treated versus IT rhASA-treated children. GM volume decline over time was steeper in children receiving low-dose (10 or 30 mg) versus high-dose (100 mg) IT rhASA. Similar effects were observed for demyelination. FA in the posterior limb of the internal capsule showed a higher trend over time in IT rhASA-treated versus children with untreated MLD, but FA parameters were not different between children receiving the low doses versus those receiving the high dose. GM volume in IT rhASA-treated children showed a strong positive correlation with 88-item Gross Motor Function Measure score over time. In some children with MLD, IT administration of high-dose rhASA may delay neurological deterioration (assessed using MRI), offering potential therapeutic benefit.

## KEYWORDS

clinical trials, enzyme replacement therapy, gross motor function, intrathecal, magnetic resonance imaging, metachromatic leukodystrophy

This is an open access article under the terms of the [Creative Commons Attribution](https://creativecommons.org/licenses/by/4.0/) License, which permits use, distribution and reproduction in any medium, provided the original work is properly cited.

© 2024 Takeda. *Journal of Inherited Metabolic Disease* published by John Wiley & Sons Ltd on behalf of SSIEM.

## 1 | INTRODUCTION

Metachromatic leukodystrophy (MLD; OMIM 250100 and 249900) is a rare, recessive lysosomal storage disease characterized by deficient activity of the arylsulfatase A (ASA) enzyme (EC 3.1.6.8).<sup>1,2</sup> This deficiency causes sulfatides to accumulate mainly in the central and peripheral nervous systems, leading to progressive demyelination and neurological deterioration.<sup>3</sup> MLD is divided into three forms: late-infantile (onset <30 months), juvenile (onset 2.5–16 years), and adult (onset >16 years).<sup>3,4</sup> All subtypes have a poor prognosis, but late-infantile MLD is the fastest-progressing form.<sup>5–7</sup> Atidarsagene autotemcel (Libmeldy, Orchard Therapeutics), an autologous hematopoietic stem cell gene therapy, has been approved in some regions for the treatment of presymptomatic patients with late-infantile or early-juvenile MLD, or early-symptomatic patients with early-juvenile MLD. However, there remains an unmet need for treatment options for symptomatic late-infantile MLD. Several therapies are under investigation, including enzyme replacement therapy with intravenous (IV) and intrathecal (IT) recombinant human ASA (rhASA).<sup>8,9</sup> A phase 1/2 trial suggested that treatment with IT rhASA may slow the motor function decline observed in MLD.<sup>9</sup>

White matter (WM) hyperintensities of T2-weighted magnetic resonance imaging (MRI) scans are used as a diagnostic tool in MLD,<sup>10,11</sup> and have been found to correlate with a worsening of motor and cognitive functions.<sup>12–15</sup> However, their utility as a marker of treatment efficacy is less clear because T2-pseudonormalization in advanced, untreated MLD has been documented.<sup>10</sup> Disruption of myelin could also disturb neuronal maturation,<sup>16</sup> and correlations between reduced gray matter (GM) volume and cognitive and motor deficits have been reported in MLD.<sup>13–15,17</sup> The assessment of GM volume, together with imaging parameters that differentiate tissue microstructure (e.g., diffusion tensor imaging [DTI]), may, therefore, be more appropriate for investigating treatment-related effects than T2-hyperintensities alone.<sup>10</sup> This retrospective analysis evaluated the effect of IT rhASA on brain tissue changes in children with MLD, as assessed using MRI.

## 2 | METHODS

### 2.1 | Standard protocol approvals, registrations, and patient consent

Both the IV rhASA (NCT00418561; NCT00633139 and extension NCT00681811) and IT rhASA (NCT01510028 and extension NCT01887938) clinical trials were conducted in accordance with the appropriate local country

regulations, the International Conference on Harmonisation of Good Clinical Practice Guidelines, and the principles of the Declaration of Helsinki.<sup>8,9</sup> Each patient's legal guardian(s) provided informed consent before study-related activities were performed.

MRI images for patients with untreated MLD were obtained as part of their clinical investigations, and parental consent for their use as part of a natural history study was obtained; the study was approved by the local ethics committee in Tübingen (401/2005).<sup>6,18</sup> The Cincinnati MR Imaging of NeuroDevelopment (C-MIND) database was approved by the Institutional Review Board at Cincinnati Children's Hospital Medical Center.<sup>19</sup> For children between 0 and 17 years of age, informed consent for their participation was provided by their legal guardian(s) and assent was provided by children older than 5 years.

### 2.2 | Study design and participants

MRI data were collected from four separate groups of children: IV rhASA-treated children with MLD,<sup>8</sup> IT rhASA-treated children with MLD,<sup>9</sup> children with untreated MLD,<sup>6,18</sup> and normally developing children<sup>19</sup> (Table 1).

#### 2.2.1 | IV rhASA phase 1/2 trial and extension

Full inclusion criteria and the study design for the IV rhASA phase 1/2 trial have been described previously.<sup>8</sup> Briefly, this single-center, open-label, nonrandomized, dose-escalation, phase 1/2 trial enrolled patients aged 12 months–6 years at screening with a confirmed diagnosis of MLD, based on accepted diagnostic criteria (deficient ASA activity and elevated sulfatide concentration).<sup>8</sup> Patients received IV rhASA (50, 100, or 200 U/kg body weight) every other week (EOW) over two consecutive 26-week periods (NCT00418561; NCT00633139). Patients who completed the phase 1/2 trial were eligible to enroll in an extension study (NCT00681811), which was discontinued owing to lack of efficacy after 24 months.

#### 2.2.2 | IT rhASA phase 1/2 trial and extension

Full inclusion criteria and the trial design for the IT phase 1/2 trial have been described previously.<sup>9</sup> Briefly, this multicenter, open-label, dose-escalation phase 1/2 trial enrolled patients with a confirmed diagnosis of MLD, based on accepted diagnostic criteria (deficient

TABLE 1 Patient groups and summary of characteristics for children included in the analysis.

	Pediatric population			
	MLD treated with IV rhASA <sup>a</sup>	MLD treated with IT rhASA	Untreated MLD	Normally developing children
Number of patients	12	24	32	156
Number of MRI scans	57	172	43	238
Sex, <i>n</i> (%)				
Male	4 (33.3)	15 (62.5)	16 (50.0)	68 (43.6)
Female	8 (67.7)	9 (37.5)	16 (50.0)	88 (56.4)
Age at first available MRI scan, years				
Median	2.9	3.1	2.2	6.3
Range	2.1–4.9	1.7–9.0	0.5–2.9	0.1–10.6
Age at MRI scan, years <sup>b</sup>				
Median	4.2	4.3	2.3	7.1
Range	2.1–7.4	1.7–10.9	0.5–6.3	0.1–10.9

<sup>a</sup>One patient was excluded from the analysis because MRI data after treatment were unavailable.

<sup>b</sup>Median age and age range across total number of scans per population.

Abbreviations: IT, intrathecal; IV, intravenous; MLD, metachromatic leukodystrophy; MRI, magnetic resonance imaging; rhASA, recombinant human arylsulfatase A.

ASA activity and elevated sulfatide concentration), who presented with symptoms of MLD by 30 months of age, were ambulatory, and displayed neurological signs of MLD at screening (NCT01510028).<sup>9</sup> Patients received 10, 30, or 100 mg IT rhASA EOW for 38 weeks. Patients who completed the phase 1/2 trial were eligible to continue receiving IT rhASA EOW as part of an ongoing extension (NCT01887938), with all patients eventually receiving 100 mg IT rhASA EOW.

Dosing between the two treated cohorts differed owing to the route of administration.

### 2.2.3 | Tübingen natural history study

Patients with a confirmed diagnosis of MLD and disease onset before 2.5 years of age were enrolled in an ongoing natural history study within the German research network LEUKONET.<sup>6</sup> Data from early-juvenile, late-juvenile, and adult MLD were also collected in the study.

### 2.2.4 | The C-MIND database

The C-MIND database contains functional neuroimaging and behavioral data from normally developing children; exclusion criteria include any chronic illness, a history of neurological or psychiatric disease, or a family history of neurological or psychiatric disease in first-degree relatives.<sup>19</sup>

## 2.3 | MRI data and image processing

Volumetric and DTI analyses were conducted centrally, at the University Children's Hospital Tübingen. GM volume was calculated from automated multispectral segmentation of high-resolution T1-weighted and axial T2-weighted images using the SPM12 software (<https://www.fil.ion.ucl.ac.uk/spm/>), as detailed previously.<sup>12</sup> Briefly, the segmentation uses both prior tissue information and tissue intensities in a modified mixture model. The volume of the resulting GM tissue maps was calculated by summing the probability values of all voxels. Fractional anisotropy (FA; a measure of WM integrity) was calculated from DTI in the regions of the posterior limb of the internal capsule (PLIC) and the centrum semiovale using the MRtrix software, version 0.3.12 ([www.mrtrix.org](http://www.mrtrix.org)). These regions were defined manually using anatomical landmarks as described in more detail previously.<sup>18</sup> Briefly, the PLIC was defined at the level of the third ventricle, and the central semiovale was defined from identification of the central sulcus, the hand knob in the precentral gyrus, and the fissura longitudinalis cerebri. These areas were selected owing to their well-defined connections to the primary motor area and their tightly packed, highly myelinated fiber structure.<sup>20,21</sup> This allows for more specificity in FA findings, given that there are few crossing fibers in the PLIC.<sup>22</sup>

Recently, it was shown that comparability of DTI parameters across different sites and scanners is relatively robust for MLD.<sup>18</sup> Identification of the pyramidal tract

was supported by color-coded eigenvector maps. DTI was performed in all studies; however, there were technical issues (a hardware malfunction) with the DTI for the IV rhASA phase 1/2 trial and extension that could not be resolved in post-processing. The resulting FA values were not comparable, and DTI data from this trial were, therefore, excluded from the analysis. Demyelination load was defined as the volume of hyperintense areas within cerebral WM in T2-weighted MRI scans and evaluated as a ratio to total WM volume. This was calculated by applying an automated intensity threshold within the WM of T2-weighted images, based on automated segmentation using the SPM12 software, as outlined previously.<sup>12</sup>

### 2.3.1 | IV rhASA phase 1/2 trial and extension

MRI data were collected at baseline and 6-monthly intervals, and acquired using a Siemens Vision 1.5 T scanner. T2-weighted anatomic images (matrix  $256 \times 256$ , field of view 320 mm, voxel size  $0.78 \times 0.78 \times 4.00 \text{ mm}^3$ ) were obtained with a spin echo sequence with echo train length 11 and echo time/repetition time = 99 ms/5400 ms. Whole-brain three-dimensional (3D) T1-weighted images were acquired using a magnetization-prepared rapid gradient-echo (MPRAGE) sequence with a voxel size of  $1 \times 1 \times 1 \text{ mm}^3$ . Owing to technical problems during acquisition, diffusion-weighted sequences were not analyzed.

### 2.3.2 | IT rhASA phase 1/2 trial and extension

MRI data were collected at baseline, at week 40, and then every 6 months in the extension study. MRI data were acquired on clinical 1.5 T and 3 T scanners at five sites (Siemens Avanto 1.5 T scanners at three sites, and a Philips Achieva 3 T scanner and a Siemens Verio 3 T scanner at one site each) using high-resolution T1-weighted MPRAGE sequences (voxel size  $1 \times 1 \times 1.2 \text{ mm}^3$ ) and axial T2-weighted sequences (voxel size  $0.43 \times 0.43 \times 3 \text{ mm}^3$ ). Diffusion sequences consisted of slices of 3 mm thickness (4 mm thickness with one scanner) and a b value of  $1000 \text{ s/mm}^2$ .

### 2.3.3 | Tübingen natural history study

MRI data were acquired on clinical 1.5 T and 3 T scanners, as detailed previously.<sup>18</sup> Specifically, 76 data sets

were assessed using a 1.5 T scanner (Vision, Sonata, Avanto Fit, Aera, Espree, Symphony, or Essenza from Siemens Healthineers; Signa from GE Healthcare; Titan from Toshiba; or Achieva or Intera from Philips Healthcare) and 35 data sets were assessed using a 3 T scanner (Skyra, Prisma Fit, Trio, or Verio from Siemens Healthineers; or Signa MR750 from GE Healthcare). Data were collected from 38 sites. MRI data consisted of conventional clinical routine images with a T1-weighted MPRAGE sequence (echo time/repetition time = 11.4 ms/4.4 ms and voxel size typically  $1 \times 1 \times 1 \text{ mm}^3$ ; in five patients, the voxel size was higher and in the range  $0.39\text{--}0.86 \times 0.39\text{--}0.86 \times 1.0\text{--}1.4 \text{ mm}^3$ ) and a T2-weighted axial sequence (typically a spin echo sequence with echo time/repetition time = 99 ms/5940 ms and voxel size  $0.78 \times 0.78 \times 4.0 \text{ mm}^3$ ; in five patients, the in-plane resolution was higher [ $0.39\text{--}0.78 \times 0.39\text{--}0.78 \text{ mm}^2$ ] and the slice thickness was in the range 3.3–7.2 mm). Different (axial) DTI sequences were used with a low b value ( $\leq 1000 \text{ s/mm}^2$ ; median b value  $1000 \text{ s/mm}^2$ , range 700–1000  $\text{s/mm}^2$ ), and spatial resolution varied between sequences (median [range] slice thickness 5 [2.0–7.2] mm).<sup>18</sup>

### 2.3.4 | The C-MIND database

MRI data were acquired on a 3 T Philips Achieva scanner, using high-resolution T1-weighted MPRAGE sequences (voxel size  $1 \times 1 \times 1 \text{ mm}^3$ ) and 3D fluid-attenuated inversion recovery (voxel size  $1 \times 1 \times 1 \text{ mm}^3$ ), as well as a diffusion-weighted sequence with b value  $1000 \text{ s/mm}^2$  (voxel size  $2 \times 2 \times 2 \text{ mm}^3$ ). Further specifications can be found here: [https://nda.nih.gov/edit\\_collection.html?id=2329](https://nda.nih.gov/edit_collection.html?id=2329); data set digital object identifier: 10.15154/1528588.

## 2.4 | Gross Motor Function Measure-88 for IT rhASA-treated children

Motor function was assessed in the IT rhASA-treated children using the 88-item Gross Motor Function Measure (GMFM-88) total score (0–100%), as described previously.<sup>9</sup> The GMFM-88 measure is a standardized observational evaluation of motor function, with 88 items categorized into five dimensions: lying and rolling; sitting; crawling and kneeling; standing; and walking, running, and jumping.<sup>23</sup> The instrument has been validated to measure longitudinal change in patients with movement disorders,<sup>24</sup> and assessments were performed by a trained physiotherapist (clinician).

## 2.5 | Statistical analyses

Characteristics of the children included in the analysis are reported as frequencies and percentages for categorical parameters, and median (range) for continuous parameters. Correlations between the MRI parameters in normally developing children and in children with MLD were tested separately by repeated-measures correlation. All patients with MLD across studies were combined for correlational analyses. In addition, correlations between MRI parameters and functional outcome in IT rhASA-treated children with MLD were assessed at baseline using Spearman rank correlation analysis and were analyzed over time by repeated-measures correlation.

### 2.5.1 | Modeling methodology

Linear mixed models were fitted to analyze the time courses of GM volume (all groups) and FA in the PLIC (normally developing children, children with untreated MLD, and IT rhASA-treated children with MLD groups only). To account for nonlinearity in GM volume, a quadratic function of the time parameter (age in analyses including normally developing children and children with untreated MLD, follow-up time from baseline in analyses including only treated children with MLD) was added to the model. To account for individual variation at baseline and for dependency across the repeated measurements within the same child, a random intercept per child and/or a random slope (for the included time variable) was included based on the Akaike information criterion. A continuous autoregressive correlation structure was also added to the model based on Akaike information criterion, to account for autocorrelation between within-subject errors.

Significance of covariates (fixed effects), including interaction between the groups and the time variable to analyze differences in time slopes, was assessed with a likelihood ratio test between the model with and without the covariate using maximum likelihood estimation (MLE). Only statistically significant covariates were included in the final model. The final coefficients were estimated using restricted MLE. Model assumptions were confirmed visually, and included normally distributed residuals, random effects, and homogeneity of variance. Random effects and model performance indicators are provided in Table S1.

Time courses of GM volume and FA in the PLIC for the different groups, with their 95% confidence intervals (CIs) as estimated by the final models, were plotted

together with the individual patient data to visualize changes over time. Data were considered statistically significant at  $p$ -values of less than 0.05. The R project (RStudio: Integrated Development for R. RStudio, Inc., Boston, MA, USA) for statistical computing version 4.0.3 with the packages “lme4,” “rmcorr,” and “ggplot2” was used for all analyses.

### 2.5.2 | Demyelination load and FA in the centrum semiovale

Time courses were plotted for demyelination load (children with MLD) and the FA in the centrum semiovale (normally developing children, children with untreated MLD, and IT rhASA-treated children). These data were not analyzed by linear mixed models owing to improper model fit and violation of the model assumptions. Instead, the time courses were visualized by locally estimated scatterplot smoothing regression curves with their 95% CIs based on the individual data.

### 2.5.3 | Comparison of IT rhASA dose groups

The effect of IT rhASA dose on GM volume, demyelination load, and FA in the PLIC and centrum semiovale were analyzed by categorizing patients receiving IT rhASA into a low-dose group (10 mg or 30 mg IT rhASA;  $n = 6$  and  $n = 6$ , respectively) and a high-dose group (100 mg IT rhASA;  $n = 12$ ).

Further descriptive statistics are reported for patients in the high-dose group who were defined post hoc as having stabilized motor function; these were patients with a GMFM-88 total score of at least 35% at baseline, which was maintained (decrease  $\leq 10\%$ ) or increased at the end of the study (40 weeks).

## 3 | RESULTS

### 3.1 | Characteristics of patients and normally developing children

In total, 510 MRI scans were obtained from 12 children with MLD treated with IV rhASA, 24 children with MLD treated with IT rhASA, 32 children with untreated MLD, and 156 normally developing children (Table 1). All treated children with MLD had repeated MRI scans; however, only single scans were available for most children with untreated MLD (21 of 32 [66%]) and normally developing children (99 of 156 [63%]).

### 3.2 | Characteristics of patients treated with 100 mg IT rhASA with stabilized motor function

Of the 12 children treated with 100 mg IT rhASA, four met the criteria for stabilized motor function. All four children continued to receive 100 mg IT rhASA EOW in the extension study for varying lengths of time. Stabilized response was maintained in the extension for three of the four children; one child showed an initial improvement in motor function but experienced a decline from the age of approximately 60 months. Median age at enrollment for these children was 39.5 months, with a median age at symptom onset of 23.0 months and a median age at diagnosis of 39.5 months. Baseline GMFM-88 total scores for these children were 39, 51, 76, and 96, and changes from baseline in GMFM-88 score to week 40 were +16.05,

−1.43, +3.83, and +0.67, respectively. At the last follow-up in the extension study, two of these children experienced an overall decline in GMFM-88 total score and the other two children maintained a stable or increased score.

### 3.3 | GM volume

Total GM volume was lower over time in all groups of children with MLD than in normally developing children of the same age (all  $p < 0.05$ ; Table 2; Figure 1A) and was lower in girls than in boys (all  $p < 0.05$ ; Table 2). An increase in GM volume would be expected with normal development; however, total GM volume declined with age in children with MLD, with the fastest decline observed in children with untreated MLD ( $p < 0.001$ ; Table 2; Figure 1A).

TABLE 2 Linear mixed models for GM volume including all children.

	Predictors (fixed effects)		
	All cohorts <sup>a</sup>	IV rhASA vs IT rhASA <sup>b</sup>	Low-dose vs high-dose IT rhASA <sup>c</sup>
Intercept, estimate (95% CI)	0.56 (0.50, 0.61) <b><math>p &lt; 0.001</math></b>	0.57 (0.51, 0.62) <b><math>p &lt; 0.001</math></b>	0.62 (0.57, 0.67) <b><math>p &lt; 0.001</math></b>
Sex, <sup>d</sup> estimate (95% CI)	−0.04 (−0.06, −0.02) <b><math>p &lt; 0.001</math></b>	−0.05 (−0.10, 0.00) <b><math>p = 0.044</math></b>	−0.07 (−0.13, −0.01) <b><math>p = 0.032</math></b>
Group estimate (95% CI)			
Normally developing children	Reference group	N/A	N/A
MLD: untreated	0.07 (−0.17, 0.31) $p = 0.549$	N/A	N/A
MLD: IV rhASA	0.36 (0.18, 0.53) <b><math>p &lt; 0.001</math></b>	N/A	N/A
MLD: IT rhASA	0.18 (0.08, 0.28) <b><math>p &lt; 0.001</math></b>	N/A	N/A
Treatment group, <sup>e</sup> estimate (95% CI)	N/A	0.07 (0.01, 0.12) <b><math>p = 0.016</math></b>	0.04 (−0.02, 0.10) $p = 0.225$

Note: Bold values are statistically significant ( $p < 0.001$ ,  $p < 0.01$ , and  $p < 0.05$ ). The fixed effects in a mixed model can be interpreted in the same way as variables in a normal linear model (i.e., given that all other variables are the same in the two children, at any given time point the GM volume of a girl is 0.04 L lower than that of a boy and the GM volume of an IT rhASA-treated child with MLD is 0.07 L higher than that of an IV rhASA-treated child with MLD). Random effects/model performance indicators are provided in Table S1.

<sup>a</sup>For the linear mixed model comparing all cohorts, age at MRI scan, squared function of age at MRI scan, interaction term between group and age at MRI scan, and interaction term between group and squared function of age at MRI scan were included in the model as significant predictors (all  $p < 0.001$ ).

<sup>b</sup>For the linear mixed model comparing IV rhASA-treated children with MLD with IT rhASA-treated children with MLD, follow-up after baseline and squared function of follow-up after baseline were included in the model as significant predictors (both  $p < 0.001$ ). Age at MRI scan and the interaction between treatment group and follow-up after baseline were not significant predictors of GM volume ( $p = 0.757$  and  $p = 0.730$ , respectively) and, therefore, were excluded from the model.

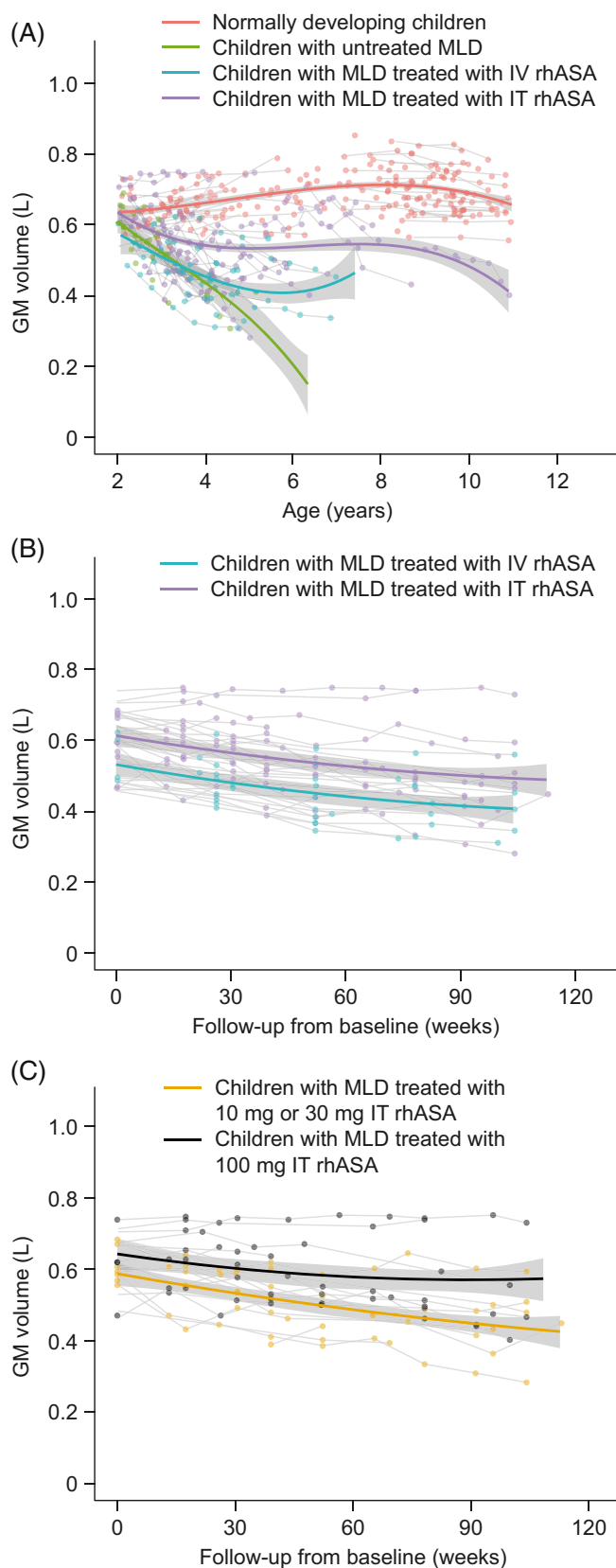
<sup>c</sup>For the linear mixed model comparing low-dose and high-dose IT rhASA-treated children with MLD, follow-up after baseline, squared function of follow-up after baseline, and interaction term between dose group and follow-up after baseline were included in the model as significant predictors ( $p < 0.001$ ,  $p < 0.001$ , and  $p = 0.035$ , respectively). Age at MRI scan was not a significant predictor of GM volume ( $p = 0.765$ ) and, therefore, was excluded from the model.

<sup>d</sup>Male sex is used as the reference group.

<sup>e</sup>For the linear mixed model comparing IV rhASA-treated children with MLD with IT rhASA-treated children with MLD, IV rhASA-treated children are used as the reference group. For the linear mixed model comparing low-dose IT rhASA-treated children with MLD with high-dose IT rhASA-treated children with MLD, the low-dose group is used as the reference group.

Abbreviations: CI, confidence interval; GM, gray matter; IT, intrathecal; IV, intravenous; MLD, metachromatic leukodystrophy; MRI, magnetic resonance imaging; N/A, not available; rhASA, recombinant human arylsulfatase A.

Total GM volume was significantly lower at any given time point during follow-up (median duration = 104 weeks)



in IV rhASA-treated children than in IT rhASA-treated children ( $p = 0.016$ ; Table 2; Figure 1B), but a statistically significant difference in rate of decline between these two groups was not observed and was not included in the final model ( $p = 0.730$ ). However, decline in total GM volume was faster in the low-dose IT rhASA group (10 or 30 mg) than in the high-dose IT rhASA group (100 mg) ( $p = 0.035$ ; Table 2; Figure 1C). Finally, individual plots indicated that treatment with 100 mg IT rhASA may have stabilized the decline in GM volume for two children (the two uppermost individual time-course plots in Figure 1C).

### 3.4 | FA in the PLIC

FA in the PLIC was significantly lower over time in untreated and IT rhASA-treated children with MLD than in normally developing children of the same age (both  $p < 0.001$ ; Table 3; Figure 2A).

FA in the PLIC showed a nonsignificant ( $p = 0.0522$ ), lower trend over time in children with untreated MLD than in IT rhASA-treated children. There was no difference in FA in the PLIC between the low-dose and high-dose IT rhASA groups ( $p = 0.791$ ; Figure 2B). There was also no statistical evidence for age differences or sex differences among all groups ( $p = 0.110$  and  $p = 0.392$ , respectively); therefore, these differences were not included in the model.

**FIGURE 1** Longitudinal comparisons of GM volume across normally developing children and untreated and treated children with MLD. The course of GM volume over time from baseline as estimated by a linear mixed model for: (A) normally developing children, children with untreated MLD, IV rhASA-treated children with MLD, and IT rhASA-treated children with MLD; (B) IV rhASA-treated children with MLD and IT rhASA-treated children with MLD; and (C) children with MLD treated with low-dose IT rhASA (10 or 30 mg) and children with MLD treated with high-dose IT rhASA (100 mg). Shadows show 95% CIs. Colored dots (measurements) and gray lines (course over time) in all graphs reflect the individual patient data. For (A), age at MRI scan and the interaction between group and age at MRI scan were significant predictors in the model, meaning that the decline over time in GM volume in patients was steeper than that observed in normally developing children. For (B) and (C), follow-up after baseline was a significant predictor in the model. For (C), the interaction between dose group and follow-up after baseline was an additional predictor of the model, meaning that the decline over time in GM volume observed in patients in the low-dose group was steeper than that observed in the high-dose group. CI, confidence interval; GM, gray matter; IT, intrathecal; IV, intravenous; MLD, metachromatic leukodystrophy; MRI, magnetic resonance imaging; rhASA, recombinant human arylsulfatase A.

**TABLE 3** Linear mixed model for FA in the PLIC including all normally developing children, children with untreated MLD, and IT rhASA-treated children with MLD.

Predictors (fixed effects)	
Intercept, estimate (95% CI)	0.73 (0.72, 0.74) <b><math>p &lt; 0.001</math></b>
Group estimate (95% CI)	
Normally developing children	Reference group
MLD: untreated	-0.35 (-0.41, -0.28) <b><math>p &lt; 0.001</math></b>
MLD: IT rhASA	-0.25 (-0.28, -0.23) <b><math>p &lt; 0.001</math></b>

*Note:* Bold values are statistically significant ( $p < 0.001$ ). The fixed effects in a mixed model can be interpreted in the same way as variables in a normal linear model (i.e., at any given time point, the FA in the PLIC in a child with untreated MLD and that in an IT rhASA-treated child with MLD are, respectively, 0.35 L and 0.25 L lower than that of a normally developing child, given that all other variables are the same between these two children). Age at MRI scan and sex were not significant predictors of FA in the PLIC ( $p = 0.110$  and  $p = 0.392$ , respectively) and, therefore, were excluded from the model. Random effects/model performance indicators are provided in Table S1.

Abbreviations: CI, confidence interval; FA, fractional anisotropy; IT, intrathecal; MLD, metachromatic leukodystrophy; MRI, magnetic resonance imaging; PLIC, posterior limb of the internal capsule; rhASA, recombinant human arylsulfatase A.

### 3.5 | Demyelination load

Demyelination loads in children with untreated MLD and IV rhASA-treated children aged 2–4 years were comparable and, in general, higher than in IT rhASA-treated children (Figure 3A). Thus, IT rhASA-treated children overall showed a lower demyelination load during follow-up (median duration = 104 weeks) than IV rhASA-treated children (Figure 3B), as did children treated with a high IT rhASA dose compared with those treated with a low IT rhASA dose (Figure 3C). Nevertheless, there was large intraindividual variation in the extent and time course of demyelination load, and CIs overlapped each other at all time points. Finally, individual plots indicated that treatment with 100 mg IT rhASA may have delayed demyelination for two patients (the two lowest individual time-course plots in Figure 3C).

### 3.6 | FA in the centrum semiovale

FA in the centrum semiovale in untreated and IT rhASA-treated children with MLD was decreased compared with that in normally developing children (Figure 4A). The

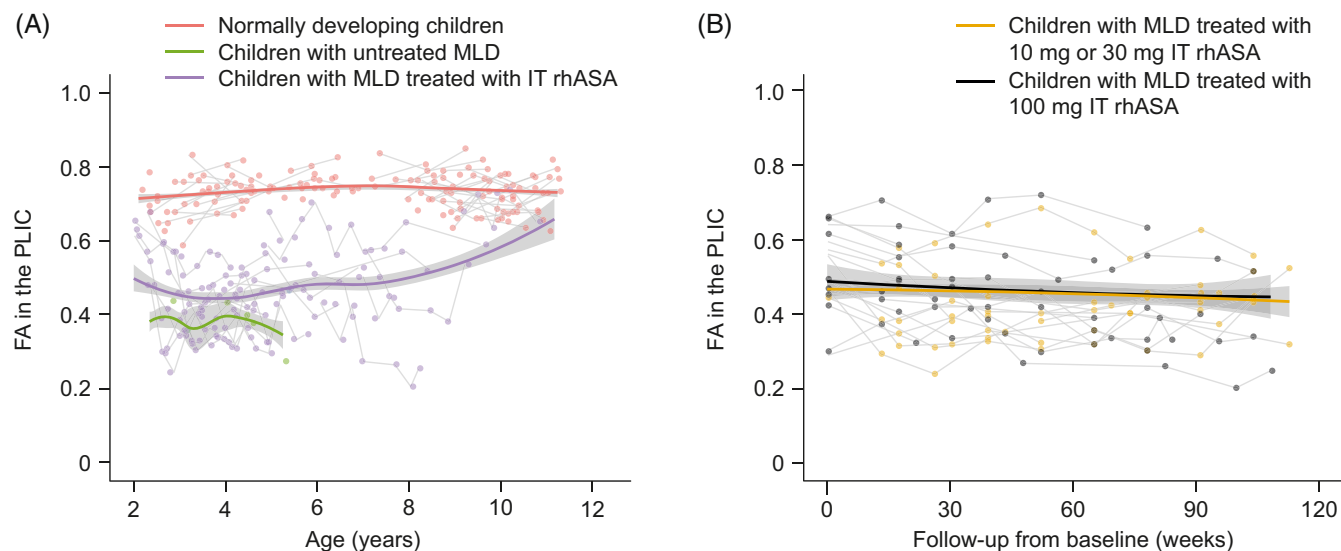
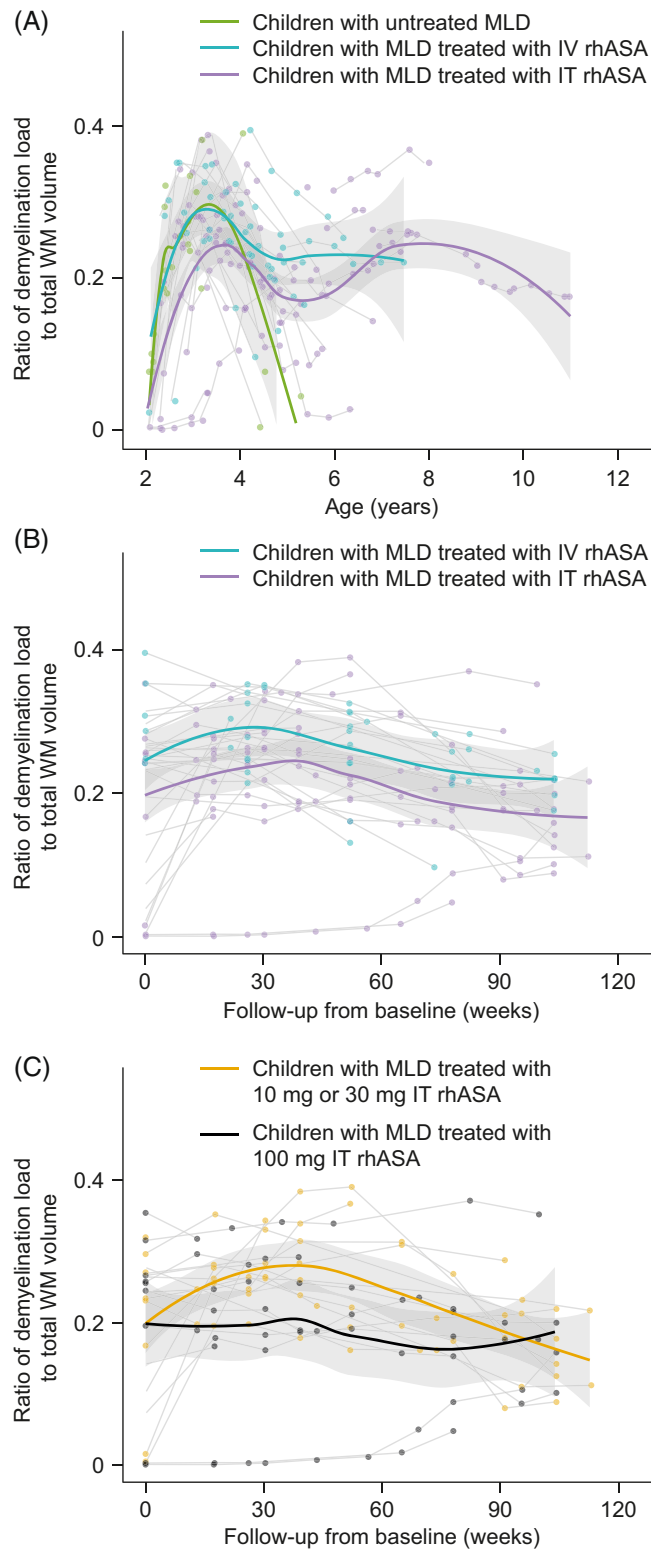


**FIGURE 2** Longitudinal comparisons of FA in the PLIC across normally developing children and untreated and IT rhASA-treated children with MLD. The course of FA in the PLIC over time from baseline as estimated by a linear mixed model for: (A) normally developing children, children with untreated MLD, and IT rhASA-treated children with MLD; and (B) children with MLD treated with low-dose IT rhASA (10 or 30 mg) and children with MLD treated with high-dose IT rhASA (100 mg). Shadows show 95% CIs. Colored dots (measurements) and gray lines (course over time) in both graphs reflect the individual patient data. CI, confidence interval; FA, fractional anisotropy; IT, intrathecal; MLD, metachromatic leukodystrophy; PLIC, posterior limb of the internal capsule; rhASA, recombinant human arylsulfatase A.



FA in the centrum semiovale was generally similar in children treated with a low or a high IT rhASA dose (Figure 4B), although two children in the high-dose group retained a relatively high FA during the follow-up period (the two highest individual time-course plots in Figure 4B).



### 3.7 | Correlations between MRI parameters

Demyelination load in children with MLD was negatively correlated with both FA in the PLIC ( $r = -0.377$ ,  $p < 0.001$ ) and FA in the centrum semiovale ( $r = -0.644$ ,  $p < 0.001$ ), but was not correlated with total GM volume ( $r = 0.140$ ,  $p = 0.084$ ). Interestingly, FA in the PLIC was positively correlated with FA in the centrum semiovale in children with MLD ( $r = 0.487$ ,  $p < 0.001$ ). FA in the PLIC was also correlated with total GM volume ( $r = 0.354$ ,  $p < 0.001$ ) in these children, whereas FA in the centrum semiovale was not ( $r = -0.029$ ,  $p = 0.744$ ). In normally developing children, FA in the PLIC and FA in the centrum semiovale were not correlated ( $r = 0.044$ ,  $p = 0.736$ ), nor were FA in the PLIC and total GM volume ( $r = 0.032$ ,  $p = 0.803$ ), but FA in the centrum semiovale and total GM volume were positively correlated ( $r = 0.377$ ,  $p < 0.001$ ).

### 3.8 | Correlations between MRI parameters and functional outcome in IT rhASA-treated children

GM volume in IT rhASA-treated children with MLD showed a strong positive correlation with GMFM-88 score over time ( $r = 0.675$ ,  $p < 0.001$ ), whereas FA in the PLIC was weakly correlated with GMFM-88 score ( $r = 0.306$ ,  $p = 0.003$ ). FA in the centrum semiovale and demyelination load were both not correlated with GMFM-88 score over time ( $r = 0.190$ ,  $p = 0.066$  and  $r = 0.041$ ,  $p = 0.670$ , respectively). However, both FA in the centrum semiovale and demyelination load were correlated with GMFM-88 score at baseline ( $r = 0.460$ ,  $p < 0.001$  and  $r = -0.266$ ,  $p = 0.004$ , respectively), although less strongly correlated than were GM volume

**FIGURE 3** Longitudinal comparisons of demyelination load across untreated and treated children with MLD. The course of demyelination load over time from baseline as estimated by LOESS regression curves for: (A) children with untreated MLD, IV rhASA-treated children with MLD, and IT rhASA-treated children with MLD; (B) IV rhASA-treated children with MLD and IT rhASA-treated children with MLD; and (C) children with MLD treated with low-dose IT rhASA (10 mg or 30 mg) and children with MLD treated with high-dose IT rhASA (100 mg). Shadows show 95% CIs based on the individual data. Colored dots (measurements) and gray lines (course over time) in all graphs reflect the individual patient data. CI, confidence interval; IT, intrathecal; IV, intravenous; LOESS, locally estimated scatterplot smoothing; MLD, metachromatic leukodystrophy; rhASA, recombinant human arylsulfatase A; WM, white matter.

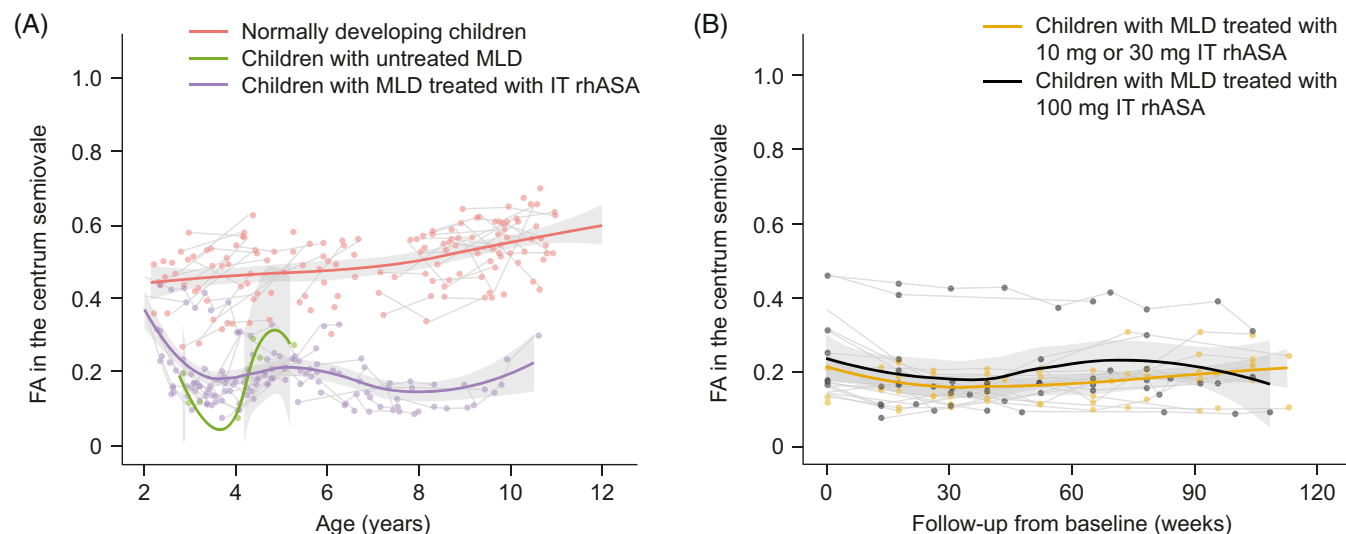


**FIGURE 4** Longitudinal comparisons of FA in the central semiovale across normally developing children and untreated and IT rhASA-treated children with MLD. The course of FA in the central semiovale over time from baseline as estimated by LOESS regression curves for: (A) normally developing children, children with untreated MLD, and IT rhASA-treated children with MLD; and (B) children with MLD treated with low-dose IT rhASA (10 or 30 mg) and children with MLD treated with high-dose IT rhASA (100 mg). Shadows show 95% CIs. Colored dots (measurements) and gray lines (course over time) in both graphs reflect the individual patient data. CI, confidence interval; FA, fractional anisotropy; IT, intrathecal; LOESS, locally estimated scatterplot smoothing; MLD, metachromatic leukodystrophy; rhASA, recombinant human arylsulfatase A.

( $r = 0.755$ ,  $p < 0.001$ ) and FA in the PLIC ( $r = 0.586$ ,  $p < 0.001$ ).

## 4 | DISCUSSION

Our findings demonstrate that patients with MLD show significant neurological deterioration across MRI parameters for both GM and WM and that treatment with 100 mg IT rhASA may delay GM atrophy. The analysis suggests this delay in GM atrophy may relate to a delay in gross motor function decline in these patients, suggesting a potential clinical benefit of treatment with the higher IT rhASA dose.

Patients with MLD showed deterioration in GM volume and FA (a measure of WM integrity) in both the PLIC and the centrum semiovale compared with normally developing children of the same age. FA in the PLIC and GM volume were positively correlated with each other in children with MLD, whereas this relationship was not observed in normally developing children. These findings are in line with previous literature: reduced GM volume at diagnosis has been observed in children with late-infantile MLD through a range of methods,<sup>12,15</sup> and decreases in cingulate, insular, and frontal lobe cortical thickness have been found to correlate with WM involvement.<sup>15</sup> Our results also extend prior MRI analyses from the IT rhASA clinical trial, in

which increases in MLD MRI severity score (indicating deterioration) were reported over time in all patients, although they were less pronounced in the 100 mg IT rhASA cohorts than in those given 10 or 30 mg IT rhASA.<sup>9</sup>

A key finding from this analysis is that GM volume was significantly lower in IV rhASA-treated patients than in IT rhASA-treated patients during follow-up, suggesting that treatment with the higher dose of IT rhASA (100 mg) may further slow the GM atrophy observed in the natural course of MLD. This slowing of GM volume atrophy in the high-dose group may translate into improved motor function, given that signs of stabilization or improved motor function were observed at the end of the trial in four patients treated with 100 mg IT rhASA EOW.<sup>9</sup> Indeed, GM volume showed a strong positive correlation with GMFM-88 score at baseline, and, more importantly, over time during the study. Therefore, GM volume is a promising MRI biomarker for the evaluation of treatment effects. In addition, the decline in GM volume over time and the correlation between GM volume and functional outcome highlight the involvement of GM in MLD, a disease previously considered to affect mainly the WM.<sup>12</sup>

Higher demyelination loads are thought to indicate greater deterioration of the myelin sheath,<sup>25</sup> and demyelination load findings showed similar trends to GM volume. We found that IT rhASA-treated children had a

lower demyelination load during follow-up from baseline than IV rhASA-treated children. In addition, lower demyelination loads were observed in children treated with 100 mg IT rhASA during follow-up than in those treated with 10 or 30 mg IT rhASA, with some individual plots indicating delayed demyelination.

These results suggest that treatment with the higher dose of IT rhASA may have beneficial effects on brain structure in symptomatic patients with MLD. Currently, there is no approved treatment for this patient population. Gene therapy has been approved in some regions for the treatment of patients with MLD, but only for pre-symptomatic patients with late-infantile or early-juvenile MLD, or early-symptomatic patients with early-juvenile MLD.<sup>26,27</sup> Patients with a diagnosis of MLD are typically from families with no prior history of the disease<sup>28</sup> and consequently receive a diagnosis after symptom onset, so there continues to be an unmet need in patients with symptomatic late-infantile MLD. Results from the phase 1/2 IT rhASA trial suggested that the 100 mg dose may provide a clinical benefit for symptomatic late-infantile MLD.<sup>9</sup> A phase 2 clinical trial evaluating the effects of 150 mg IT rhASA delivered weekly is underway and aims to provide further information on the efficacy of IT rhASA.

In contrast to GM volume, differences in FA values in the PLIC between patients treated with IT rhASA and untreated patients did not reach significance for the whole cohort. Furthermore, a steeper decline in FA in the PLIC and in the centrum semiovale was not observed for patients in the low-dose IT rhASA groups (10 or 30 mg) compared with the high-dose IT rhASA group (100 mg), in contrast to data reported for GM volume. This is also supported by the finding that the correlations between GMFM-88 score and FA at the PLIC at baseline and over time are weaker than the correlations between GMFM-88 score and GM volume. Insight into differences in the GM volume, demyelination load, and FA findings may be gained from *in vitro* studies, in which neurons displayed a higher uptake of recombinant enzymes than oligodendrocytes.<sup>29</sup> Mature oligodendrocytes are crucial for myelin repair and thereby for limiting axon degeneration,<sup>30</sup> so the limited uptake by these cells may translate into less pronounced improvements in imaging parameters that are sensitive to changes in myelin, such as FA. However, caution must be taken with the interpretation of FA parameters, because they can be influenced by microstructural variations in crossing fibers.<sup>31,32</sup> Although we selected areas of clinical relevance and suitability for FA analyses, more sensitive, tissue-specific WM parameters for WM microstructure than FA may be required to characterize microstructural properties accurately and to assess functionally relevant treatment effects.<sup>33,34</sup>

Although this study has progressed our understanding of the potential treatment effects of IT rhASA on neurological structure, there are several limitations. First, owing to the nature of rare diseases, patient populations were small. Specifically, subdividing the population of patients treated with IT rhASA into low- and high-dose groups resulted in particularly small samples for these analyses and may limit the power of these results. Future work is necessary to confirm these findings in larger cohorts. In addition, data were collected from four independent studies, which introduced variability in MRI data acquisition protocols and data availability. For instance, DTI was not included for the IV rhASA clinical trial owing to technical sequence issues, so we do not know how WM microstructure in this group differed from that in untreated patients or patients receiving IT rhASA. However, IV rhASA treatment is not expected to result in any significant changes to WM microstructure: IV rhASA did not affect central nervous system symptoms in the clinical trial, suggesting that it cannot cross the blood-brain barrier in therapeutic quantities.<sup>8</sup> Furthermore, variability in patient demographics and stage of disease might also be expected when comparing four separate cohorts, particularly for the natural history cohort, which used less-stringent inclusion criteria, and the healthy cohort, which would likely show variability inherent to normal development.<sup>35</sup> Visual inspection of the graphs also suggests that patients receiving 100 mg IT rhASA doses had less-advanced disease at baseline than most patients in all other groups, indicated by better MRI parameters and motor function. However, our statistical modeling approach took account of several confounding factors across studies to control for this variation. We included a random intercept and a random time slope to control for individual variation in MRI parameters at baseline and disease course, and included covariates when significant, including age at MRI, sex, and follow-up duration for patients.

It is encouraging that the FA in the centrum semiovale and demyelination load findings followed the same pattern as FA at the PLIC and GM volume, respectively. The trajectory of demyelination load in children with untreated late-infantile MLD is known to increase initially but to decrease or to “normalize” in the advanced stages of the disease.<sup>10</sup> This T2-pseudonormalization may occur owing to the migration and accumulation of enzyme-deficient myelin and sulfatide-laden phagocytes, causing increases in tissue density and a subsequent drop in the T2 signal.<sup>10</sup> Consequently, lower demyelination load could be misinterpreted as a therapeutic response if taken in isolation, so it should not be used as a biomarker for disease severity in advanced late-infantile MLD. A slower/delayed initial increase in

demyelination load, together with the lack of/delayed decrease in demyelination load reported here as well as corroboration with delayed GM atrophy, suggests an observed treatment effect of IT rhASA rather than a misinterpretation of T2-pseudonormalization. In addition, high demyelination load at an early disease stage and low demyelination load at a later disease stage due to T2-pseudonormalization may explain the lack of correlation between demyelination load and GMFM-88 score over time, whereas a correlation between demyelination load and GMFM-88 score at baseline was observed in this analysis.

Future work could benefit from the inclusion of other imaging parameters that provide complementary information on WM microstructure, such as myelin water fraction or magnetization transfer ratio.<sup>10,33</sup> *N*-acetylaspartate (NAA) levels in magnetic resonance spectroscopy may also be a more sensitive biomarker for WM microstructure early in the disease course.<sup>9,33</sup> NAA levels are a known marker for neuronal and axonal loss, have been shown to decrease with increasing progression of MLD, and strongly correlate with cognitive (and motor) function in these patients.<sup>36</sup> Furthermore, NAA levels have been found to predict outcomes following hematopoietic stem cell transplantation in patients with juvenile or adult MLD.<sup>37</sup> In line with these findings, the phase 1/2 trial of IT rhASA showed a less pronounced decrease in the NAA/creatinine ratio for higher-dosing groups, suggesting a delay in neuroaxonal loss.<sup>9</sup> Taken together, these results support the use of multimodal MRI protocols when evaluating treatment efficacy in clinical trials.<sup>10,12</sup>

## 5 | CONCLUSIONS

Treatment with IT rhASA may show promise in delaying the deterioration of GM volume in patients with MLD, which may translate to stabilized motor function for selected patients. The phase 2 clinical trial currently underway (NCT03771898) aims to provide further information on the efficacy of IT rhASA.

### AUTHOR CONTRIBUTIONS

Samuel Groeschel, Shanice Beerepoot: conception or design of the study; acquisition analysis and interpretation of data; drafting and revising the manuscript. Lucas Bastian Amedick, Ingeborg Krägeloh-Mann, Jing Li, David A. H. Whiteman, Nicole I. Wolf, John D. Port: analysis and interpretation of data; drafting and revising the manuscript.

### ACKNOWLEDGMENTS

We thank Rigshospitalet, Copenhagen, Denmark (Dr Merete Ljungberg and Dr Lars Hanson) and

Copenhagen University Hospital for their contributions to the MRI data collection.

Data presented in this work were obtained from the database known as Cincinnati MR Imaging of NeuroDevelopment (C-MIND), provided by the Pediatric Functional Neuroimaging Research Network. This network and the resulting C-MIND database were supported by contract from the Eunice Kennedy Shriver National Institute of Child Health and Human Development (HHSN275200900018C). The database has now merged with the National Institute of Mental Health (NIMH) Data Archive (NDA). The NDA is a collaborative informatics system created by the National Institutes of Health (NIH) to provide a national resource to support and to accelerate research in mental health. Data set identifier(s): DOI [10.15154/1528308](https://doi.org/10.15154/1528308). This manuscript reflects the views of the authors and may not reflect the opinions or views of the NIH or of the submitters submitting original data to the NDA.

Samuel Groeschel, Shanice Beerepoot, Ingeborg Krägeloh-Mann, and Nicole I. Wolf are members of the European Reference Network for Rare Neurological Diseases (ERN-RND), project ID 739510.

Samuel Groeschel was supported by a research grant from the German Research Foundation (GR 4688/2-2). Open Access funding was enabled and organized by Projekt

### FUNDING INFORMATION

This analysis and the NCT01510028, NCT00418561, NCT01887938, NCT00633139, and NCT00681811 studies were funded by Shire (a Takeda company). Medical writing support was provided by Emma Davies PhD of Oxford PharmaGenesis, Oxford, UK, and was funded by Takeda Development Center Americas, Inc.

### CONFLICT OF INTEREST STATEMENT

Samuel Groeschel received an institutional research grant from Shire (a Takeda company) for this analysis and conducted adviser activities for Clario, Homology Medicines, Orchard Therapeutics, and Passage Bio, without personal payments.

Shanice Beerepoot and Lucas Bastian Amedick report no disclosures.

Ingeborg Krägeloh-Mann received travel expenses from Shire (a Takeda company).

Jing Li was a full-time employee of Takeda at the time of the analysis.

David A. H. Whiteman was a full-time employee of Takeda and a stockholder of Takeda Pharmaceuticals Company Limited at the time of the analysis.

Nicole I. Wolf received travel expenses from Orchard Therapeutics and is a consultant for Ionis, Lilly, Passage

Bio, Sana Biotech, Takeda, and Vigil Neuro, without personal payments.

John D. Port is contracted by Shire (a Takeda company) to perform blinded imaging scoring and spectroscopy analysis of MRI and magnetic resonance spectroscopy data.

### DATA AVAILABILITY STATEMENT

Takeda Development Center Americas, Inc. does not plan to share data supporting the results reported in this article because there is a reasonable likelihood that individual patients could be reidentified, owing to the limited number of study sites/participants.

### ETHICS STATEMENT

Both IV rhASA and IT rhASA clinical trials were conducted in accordance with the appropriate local country regulations, the International Conference on Harmonisation of Good Clinical Practice Guidelines, and the principles of the Declaration of Helsinki. The natural history study was approved by the local ethics committee in Tübingen (401/2005), and the Cincinnati MR Imaging of NeuroDevelopment (C-MIND) database was approved by the Institutional Review Board at Cincinnati Children's Hospital Medical Center.

### INFORMED CONSENT

No patient-identifying information is included in this article.

### ANIMAL RIGHTS

This article does not contain any studies with animal subjects performed by any of the authors.

### ORCID

Samuel Groeschel  <https://orcid.org/0000-0002-2706-7163>

Shanice Beerepoot  <https://orcid.org/0000-0003-2945-6784>

David A. H. Whiteman  <https://orcid.org/0000-0001-6383-9338>

John D. Port  <https://orcid.org/0000-0002-4237-7776>

### REFERENCES

- Gieselmann V, Krägeloh-Mann I. Metachromatic leukodystrophy. In: Valle D, Beaudet AL, Vogelstein B, Kinzler K, Antokarakis S, Ballabio A, eds. *Scriver's Online Metabolic and Molecular Bases of Inherited Disease*. McGraw-Hill; 2018. Accessed April 24, 2023. <https://ommbid.mhmedical.com/content.aspx?sectionid=225546629&bookid=2709&Resultclick=2>
- Gomez-Ospina N. Arylsulfatase A deficiency. In: Adam MP, Feldman J, Mirzaa GM, et al., eds. *GeneReviews*<sup>®</sup>. University of Washington; 2017. Accessed April 24, 2023. <https://www.ncbi.nlm.nih.gov/books/NBK1130/>
- Gieselmann V. Metachromatic leukodystrophy: genetics, pathogenesis and therapeutic options. *Acta Paediatr*. 2008;97(s457):15-21.
- van Rappard DF, Boelens JJ, Wolf NI. Metachromatic leukodystrophy: disease spectrum and approaches for treatment. *Best Pract Res Clin Endocrinol Metab*. 2015;29(2):261-273.
- Fumagalli F, Zambon AA, Rancoita PMV, et al. Metachromatic leukodystrophy: a single-center longitudinal study of 45 patients. *J Inherit Metab Dis*. 2021;44(5):1151-1164.
- Kehrer C, Elgün S, Raabe C, et al. Association of age at onset and first symptoms with disease progression in patients with metachromatic leukodystrophy. *Neurology*. 2021;96(2):e255-e266.
- Mahmood A, Berry J, Wenger DA, et al. Metachromatic leukodystrophy: a case of triplets with the late infantile variant and a systematic review of the literature. *J Child Neurol*. 2010;25(5):572-580.
- í Dali C, Groeschel S, Moldovan M, et al. Intravenous arylsulfatase A in metachromatic leukodystrophy: a phase 1/2 study. *Ann Clin Transl Neurol*. 2020;8(1):66-80.
- í Dali C, Sevin C, Krägeloh-Mann I, et al. Safety of intrathecal delivery of recombinant human arylsulfatase A in children with metachromatic leukodystrophy: results from a phase 1/2 clinical trial. *Mol Genet Metab*. 2020;131(1-2):235-244.
- Martin P, Hagberg GE, Schultz T, et al. T2-pseudonormalization and microstructural characterization in advanced stages of late-infantile metachromatic leukodystrophy. *Clin Neuroradiol*. 2021;31(4):969-980.
- Schoenmakers DH, Beerepoot S, Krägeloh-Mann I, et al. Recognizing early MRI signs (or their absence) is crucial in diagnosing metachromatic leukodystrophy. *Ann Clin Transl Neurol*. 2022;9(12):1999-2009.
- Groeschel S, í Dali C, Clas P, et al. Cerebral gray and white matter changes and clinical course in metachromatic leukodystrophy. *Neurology*. 2012;79(16):1662-1670.
- Groeschel S, Kehrer C, Engel C, et al. Metachromatic leukodystrophy: natural course of cerebral MRI changes in relation to clinical course. *J Inherit Metab Dis*. 2011;34(5):1095-1102.
- Strölin M, Krägeloh-Mann I, Kehrer C, Wilke M, Groeschel S. Demyelination load as predictor for disease progression in juvenile metachromatic leukodystrophy. *Ann Clin Transl Neurol*. 2017;4(6):403-410.
- Tillema J-M, Derks MGM, Pouwels PJW, et al. Volumetric MRI data correlate to disease severity in metachromatic leukodystrophy. *Ann Clin Transl Neurol*. 2015;2(9):932-940.
- Brady ST, Witt AS, Kirkpatrick LL, et al. Formation of compact myelin is required for maturation of the axonal cytoskeleton. *J Neurosci*. 1999;19(17):7278-7288.
- Eichler F, Grodd W, Grant E, et al. Metachromatic leukodystrophy: a scoring system for brain MR imaging observations. *AJNR Am J Neuroradiol*. 2009;30(10):1893-1897.
- Amedick LB, Martin P, Beschle J, et al. Clinical significance of diffusion imaging in metachromatic leukodystrophy. *Neuropediatrics*. 2023;54(4):244-252.
- National Institute of Mental Health Data Archive. Cincinnati MR Imaging of Neurodevelopment (C-MIND). 2020. Accessed May 3, 2022. [https://nda.nih.gov/edit\\_collection.html?id=2329](https://nda.nih.gov/edit_collection.html?id=2329)
- Groeschel S, Kühl JS, Bley AE, et al. Long-term outcome of allogeneic hematopoietic stem cell transplantation in patients with juvenile metachromatic leukodystrophy compared with

- nontransplanted control patients. *JAMA Neurol.* 2016;73(9):1133-1140.
21. Yagishita A, Nakano I, Oda M, Hirano A. Location of the corticospinal tract in the internal capsule at MR imaging. *Radiology.* 1994;191(2):455-460.
  22. Lazar M, Jensen JH, Xuan L, Helpert JA. Estimation of the orientation distribution function from diffusional kurtosis imaging. *Magn Reson Med.* 2008;60(4):774-781.
  23. Russell DJ, Rosenbaum P, Wright M, et al. *Gross Motor Function Measure (GMFM-66 & GMFM-88) User's Manual.* Mac Keith Press; 2002.
  24. Lundkvist Josenby A, Jarnlo G-B, Gummesson C, Nordmark E. Longitudinal construct validity of the GMFM-88 total score and goal total score and the GMFM-66 score in a 5-year follow-up study. *Phys Ther.* 2009;89(4):342-350.
  25. Clas P, Groeschel S, Wilke M. A semi-automatic algorithm for determining the demyelination load in metachromatic leukodystrophy. *Acad Radiol.* 2012;19(1):26-34.
  26. European Medicines Agency. *Libmeldy (atidarsagene autotemcel) summary of product characteristics.* 2021. Accessed May 14, 2021. <https://www.ema.europa.eu/en/medicines/human/EPAR/libmeldy>
  27. Fumagalli F, Calbi V, Natali Sora MG, et al. Lentiviral haematopoietic stem-cell gene therapy for early-onset metachromatic leukodystrophy: long-term results from a non-randomised, open-label, phase 1/2 trial and expanded access. *Lancet.* 2022;399(10322):372-383.
  28. Rosenberg JB, Kaminsky SM, Aubourg P, Crystal RG, Sondhi D. Gene therapy for metachromatic leukodystrophy. *J Neurosci Res.* 2016;94(11):1169-1179.
  29. Kaminski D, Yaghootfam C, Matthes F, Reßing A, Gieselmann V, Matzner U. Brain cell type-specific endocytosis of arylsulfatase A identifies limitations of enzyme-based therapies for metachromatic leukodystrophy. *Hum Mol Genet.* 2020;29(23):3807-3817.
  30. Marangon D, Boccazzi M, Lecca D, Fumagalli M. Regulation of oligodendrocyte functions: targeting lipid metabolism and extracellular matrix for myelin repair. *J Clin Med.* 2020;9(2):470.
  31. Figley CR, Uddin MN, Wong K, Kornelsen J, Puig J, Figley TD. Potential pitfalls of using fractional anisotropy, axial diffusivity, and radial diffusivity as biomarkers of cerebral white matter microstructure. *Front Neurosci.* 2021;15:799576.
  32. Groeschel S, Tournier JD, Northam GB, et al. Identification and interpretation of microstructural abnormalities in motor pathways in adolescents born preterm. *Neuroimage.* 2014;87:209-219.
  33. Groeschel S, Hagberg GE, Schultz T, et al. Assessing white matter microstructure in brain regions with different myelin architecture using MRI. *PLoS One.* 2016;11(11):e0167274.
  34. Riffert TW, Schreiber J, Anwander A, Knösche TR. Beyond fractional anisotropy: extraction of bundle-specific structural metrics from crossing fiber models. *Neuroimage.* 2014;100:176-191.
  35. Mills KL, Siegmund KD, Tamnes CK, et al. Inter-individual variability in structural brain development from late childhood to young adulthood. *Neuroimage.* 2021;242:118450.
  36. í Dali C, Hanson LG, Barton NW, Fogh J, Nair N, Lund AM. Brain N-acetylaspartate levels correlate with motor function in metachromatic leukodystrophy. *Neurology.* 2010;75(21):1896-1903.
  37. van Rappard DF, Klauser A, Steenweg ME, et al. Quantitative MR spectroscopic imaging in metachromatic leukodystrophy: value for prognosis and treatment. *J Neurol Neurosurg Psychiatry.* 2018;89(1):105-111.

## SUPPORTING INFORMATION

Additional supporting information can be found online in the Supporting Information section at the end of this article.

**How to cite this article:** Groeschel S, Beerepoot S, Amedick LB, et al. The effect of intrathecal recombinant arylsulfatase A therapy on structural brain magnetic resonance imaging in children with metachromatic leukodystrophy. *J Inherit Metab Dis.* 2024;47(4):778-791. doi:[10.1002/jimd.12706](https://doi.org/10.1002/jimd.12706)